Atomic-scale STEM-EELS Mapping across Functional Interfaces

Christian Colliex, Laura Bocher, Francisco de la Peňa, Alexandre Gloter, Katia March, and Michael Walls

Aberration-corrected scanning transmission electron microscopes can now raster Angström-sized electron probes across cross-sectional foils with interfaces parallel to the incident beam. Bright and annular dark field images deliver views of the structural arrangement of the atomic columns across such interfaces. In parallel, electron energy-loss spectroscopy is efficient for recording the electronic response of the specimen with a high level of spatial and energy resolution. It thus provides maps, atomic column by atomic column, of the nature, and in some cases of the bonding state, of the atoms across artificially grown heterolayers for electronics, spintronics, and photonics components.

INTRODUCTION

Over the past few years, novel electron transport behaviors have been observed under electric and/or magnetic fields on hetero-structures grown one atomic layer at a time. Among them, let us mention the systems which have attracted the most consideration, the magnetic tunnel junctions (MTJ)[1,2] for spintronics applications. It has rapidly become evident that interface phenomena play a major role in the origin of their remarkable properties.

Consequently, epitaxially grown oxide-based multilayers have been the subject of many detailed investigations with the goal of relating the ultimate structure and chemistry at the atomic-scale with the appearance and/or the destruction of spectacular properties. Within this context, the recent advances in electron microscopy techniques and methods play a crucial role. The most striking new applications arise from the significant progress in spatial resolution due to the introduction of aberration correctors[3,4] and in the broad development of the spectrum-image acquisition of multidimensional data, particularly for electron energy-loss spectroscopy (EELS).[5,6]

The present manuscript reviews key features of the newly accessible instrumentation, techniques, and methods together with the associated advances in performance.

TECHNIQUES AND METHODS

The fine electron probe of a scanning transmission electron microscope (STEM) is rastered over the surface of the thin specimen prepared as a section across the grown succession of layers, so that the interfaces (and atomic columns) of interest can be aligned parallel to the direction of the primary beam. Using selected tilt orientations, these columns are often made of a single atomic species. The electrons travel along them and interact with their constitutive atoms, so that they are scattered to various angles and lose part of their energy.

Over the past few years in our laboratory, two generations of STEM microscopes, both with and without C_s aberration correctors, have been used. The primary electron probe size has been significantly reduced with the latest generation of corrected UltraSTEM (Nion Co.) microscopes (down to about 0.1 nm), as compared with the 0.5 nm probe diameter available with the Vacuum Generators HB501 instrument used for the earlier experiments a few years ago.

In the spectrum-image mode (illustrated in Figure 1), for each position of the probe on the specimen (i.e., for each pixel of an image), the signals corresponding to electrons scattered to large angle into an annular detector and to those responsible for an energy loss spectrum over a given energy range, are simultaneously recorded. Within a short time, typically a few tens of milliseconds in the experiments reported here, the structural and topographic information carried by the high angle annular dark field (HAADF) signal, as well as the chemical and electronic information in the electron energy-loss spectroscopy (EELS) spectrum, can be recorded for a given pixel, the position of which has been defined with a very high level (typically a sub-Angström) accuracy. This unique combination of signals offers the possibility of moni-

How would you…

…describe the overall significance of this paper?

New possibilities in analytical transmission electron microscopy including aberration correctors, spectrometers, and data processing, can now provide maps of the structure and of the chemistry atomic column per atomic column. It thus constitutes a major step for assisting us in the comprehension of bonding between two crystals at the atomic scale.

…describe this work to a materials science and engineering professional with no experience in your technical specialty?

The functional properties exhibited by new devices made of heterostructures are often governed by the detailed organization of atoms on both sides of an interface; it is now possible to visualize and analyze them directly with the most recent generation of electron microscopes.

…describe this work to a layperson?

This paper describes how to see and recognize atoms building functional interfaces with new properties.

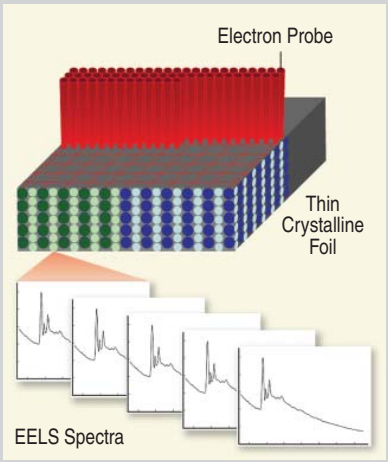

Figure 1. Principle of data acquisition of a spectrum-image across an interface, the specimen being oriented so that the interface between the A crystal (on the left with atomic columns in green) and the B crystal (on the right with atomic columns in blue) is parallel to the direction of propagation of the electron beam. For each position of the probe, one or several EELS spectra are acquired simultaneously with an annular dark field signal [adapted from C. Colliex, *Nature News & Views*, 450 (2007), p. 622].

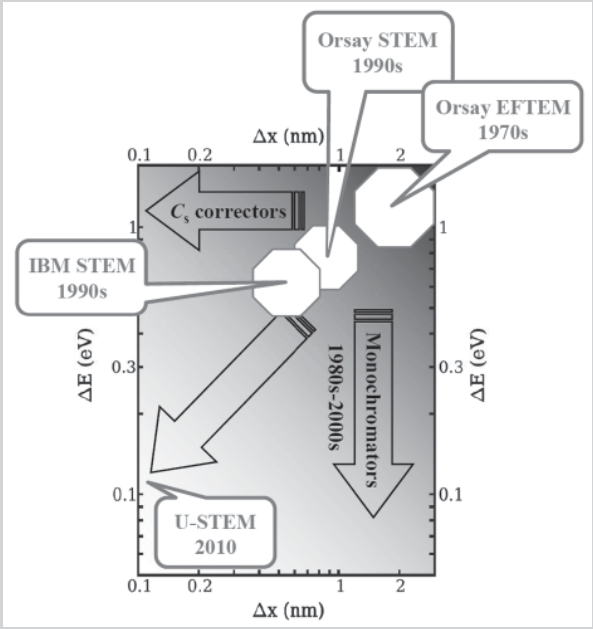

Figure 3. Evolution of the performance (spatial and energy resolution) demonstrated by EELS-STEM instruments over the past three decades and future projection. One must also emphasize that these technical steps have to be accompanied in parallel by developments in data processing and in modeling tools, in order to extract the maximum amount of information from the huge data sets now acquired by the instruments.

toring the chemical composition (presence of characteristic signals in the EELS spectrum) and the electronic state, or valence state, of the atoms (fine structures on the EELS edges), atomic column by atomic column.

To convert these large data sets (typically 1 kByte per pixel) into images or maps, many pieces of software have been implemented. One can process each spectrum individually (for example subtracting a background under an edge) and plot the energy position or intensity of identified edges or lines. More refined approaches consist of simulating the experimental spectra with the best combination of model curves and/or standards and to estimate the weight of these components in each experimental spectrum. As an example, we have introduced the use of multiple least square (MLS) fitting methods for identifying the variations of the edges' fine structures in complex boron nitride samples and in particular for mapping the bonding types of boron in these samples.[7] Alternative and/or complementary approaches, based on multivariate statistical techniques (principal component analysis,[8] independent component analysis[9]), consider the recorded set of data as a whole in order to identify its main components.

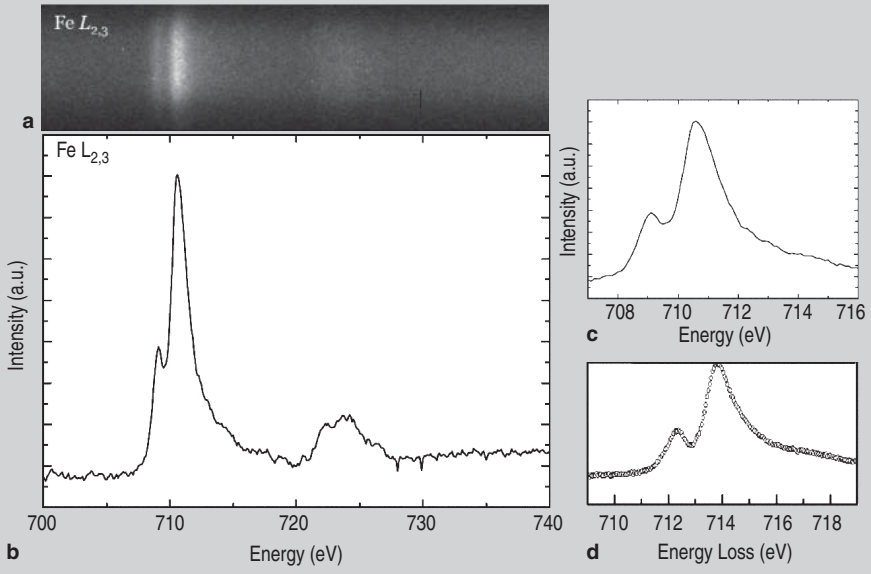

Figure 2. (a) and (b), respectively, 2D and 1D EELS spectra of Fe $L_{2,3}$ edges for α-Fe_2O_3, (c) ELNES spectrum of the Fe L_3 edge compared with (d) the corresponding monochromated spectrum from [Arnold et al. *Chem. Mat.* 21 (2009), p. 635]. The present EELS spectra were acquired on the Nion SuperSTEM microscope with a convergence semi-angle of 35 mrad, an energy dispersion of 0.1 eV/channel, a total recording time of 10 s. The 2D EELS spectrum is the image of the spectrum on the detector at the exit of the spectrometer. The vertical axis corresponds to the q momentum (the EELS collection semi-angle is 50 mrad).

As mentioned above, fine structures on a characteristic edge convey a lot of useful information. It is therefore essential to record them with both optimal energy resolution and signal-to-noise ratio. These considerations may be conflicting when using a monochromator, as the introduction of a narrow energy selection slit reduces the amount of current available on the specimen. Generally speaking, it is necessary to optimize all experimental parameters which govern the experimental resolution and the intensity of the core-loss signals: brightness and natural width of the electron source, reduction of the different types of instabilities, coupling between specimen exit surface and entrance of the EELS spectrometer, optical coupling between spectrometer exit and detector, charac-

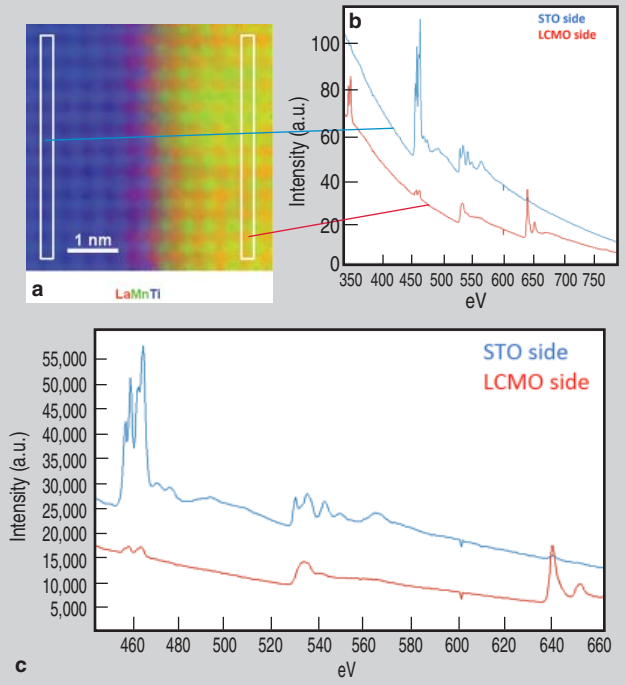

Figure 4. (a) Atomic-resolution elemental maps at a STO-LCMO interface grown along the [100] direction. For each pixel, the characteristic signal for each edge is measured after background subtraction and the intensity of the three clearly distinct elements on this map is translated into a three-color code: La (red), Mn (green), and Ti (blue). Note the anticorrrelation between Mn and Ti column positions on the manganite side. As for the Ca map (not shown here), the bright spots are superposed in position with those of the La columns, confirming the substitution process. (b) Summed spectra from the regions in the white boxes on either side of the interface showing the whole range of used energy loss with five characteristic signals from lower to higher energy loss values: Ca L_{23}, Ti L_{23}, O K, Mn L_{23}, and La M_{45}. (c) Zoom on Ti, O, and Mn edges exhibiting the fine structures which can be used for refined bond, coordination or valence mappings. *[Study performed in collaboration with Barcelona University and Barcelona Materials Institute, Spain.]*

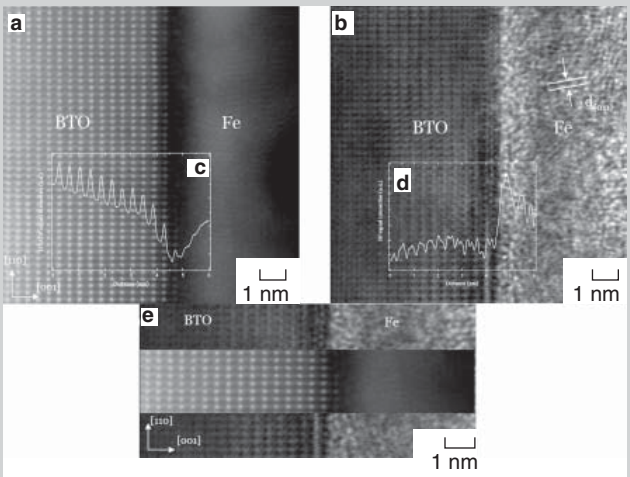

Figure 5. (a) and (b) Simultaneously-acquired atomically-resolved STEM-HAADF and STEM-BF images of the BTO/Fe interface, respectively; (c) and (d), intensity profiles of the HAADF and BF signals across the interface, respectively; (e) STEM-BF/HAADF/BF overlayered images to guide the eye regarding the atomic structure at the interface. The STEM-BF and HAADF intensity profiles are intended to match with the scale of the corresponding background images. *[Study performed in collaboration with the Unité Mixte de Physique CNRS-Thalès (UMR 137), Palaiseau, France.]*

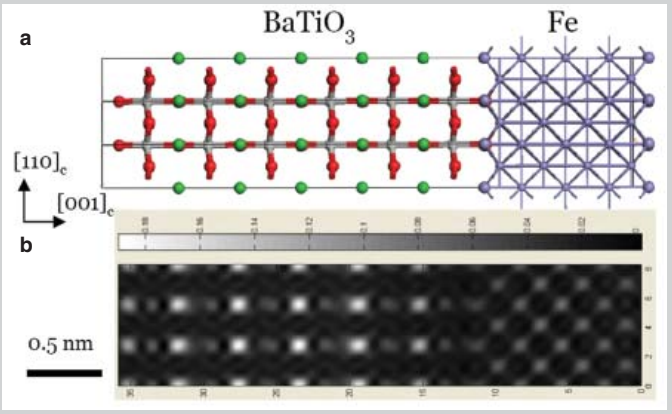

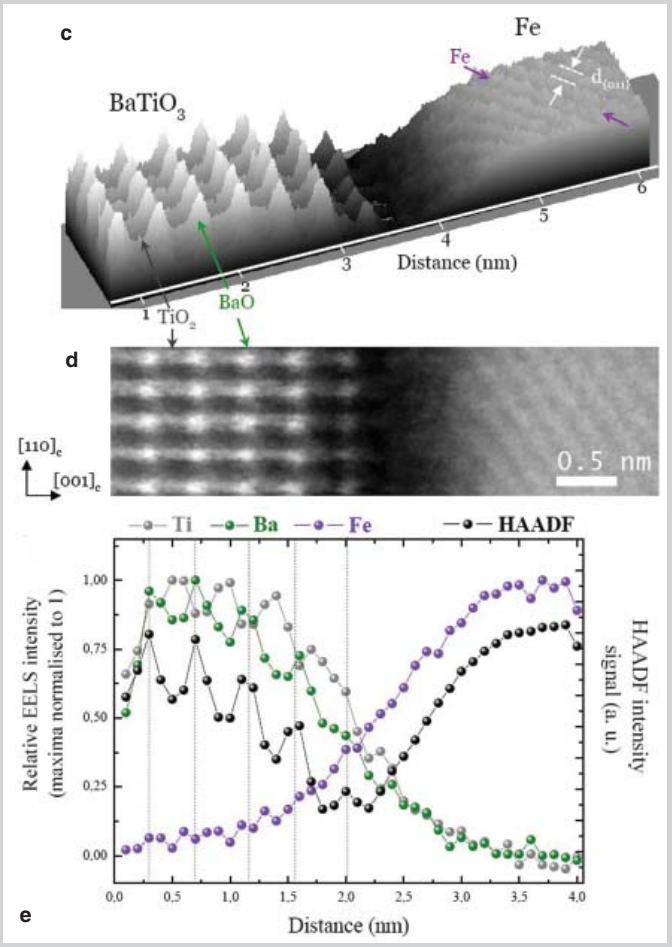

Figure 6. (a) Structural model of the $BaTiO_3$/Fe interface, and (b) corresponding simulated HAADF image using the multislice method (QSTEM software). (d) Atomically-resolved STEM-HAADF image of the rastered BTO/Fe area, (c) the corresponding 3D profile, and (e) the correlated elemental profiles across the studied BTO/Fe interface combined with the HAADF profile. The chemical profiles were extracted after a power-law background subtraction. In (a), Ba, Ti, O, and Fe atoms correspond to green, grey, red, and violet spheres, respectively.

teristics of the charge-coupled device (CCD) camera, etc. An alternative approach also consists of using deconvolution procedures.[10] Figure 2 shows detailed EELS fine structures on the Fe $L_{2,3}$ edges for a hematite Fe_2O_3 specimen, without any a posteriori processing. They exhibit a joint quality in S/N and in energy resolution sufficient for monitoring electron charge transfer levels of a few tenths of an electron on neighboring atomic sites.

To summarize the major trends in instrumentation progress, Figure 3 plots the gains in spatial and energy resolutions (typically of one order of magnitude, from nm to Å in space and from a few eV to a few 0.1 eV in energy), which have occurred over the past three or four decades. It also underlines the timescale which has been required for reaching these new levels of performance.

MAPPING ACROSS INTERFACES

Atomically-resolved elemental mapping by core-loss EELS spectrum-imaging was demonstrated quasi simultaneously, a couple of years ago, by three groups using the spectrum-image approach described above. The first two studies[11,12] focused on element-selective imaging of a perfect crystalline structure, the second one in particular used a Cs corrected STEM and compared their experimentally extracted maps with simulations in order to explain possible deviations with respect to a straight intuitive interpretation. However, the first application to interfaces was published by Muller et al. in 2008.[13] It dealt with the two-dimensional elemental mapping of a spin-polarized MTJ made of a thin strontium titanate (STO for $SrTiO_3$) insulating barrier, a few atomic layers thick, between two manganite perovskite magnetic electrodes (LSMO for $La_{2/3}Sr_{1/3}MnO_3$). This detailed study focusing on both interfaces provides elemental identification and visualization of the electron structure governed by crystal field and electron transfer. In their paper,[13] Muller et al. have shown in particular that interface intermixing extends over typically one atomic plane and symmetrically for the B-type components (Ti and Mn), while it is slightly asymmetric for the A-type components (La and Sr), i.e. very abrupt on the bottom interface (along the growth direction) and spread over a couple of layers on the top one.

However, these MTJs exhibit different behaviors depending on the detailed growth conditions,[14] such as the deposition technique used (e.g., pulse-laser or rf-sputtering), the operating parameters, the substrate crystal orientation, etc. Many questions remain unanswered before junctions for practical use at room temperature can reliably be grown. As an example (see Reference 15), we have undertaken a detailed atomic-scale study of STO/LCMO interfaces (C is for Ca which can be used instead of Sr in the manganite perovskite electrodes), with different crystallographic orientation of the substrate (001) or (110). Figure 4 illustrates the type of information on which the extended analysis, see Reference 16 for full report, is performed: (i) a map of the elemental distribution based on the weight of the characteristic Ti, Mn, and La peaks in the different pixels; (ii) a selection of spectra summed on all pixels within the areas identified on the map, in order to provide a hint of the available SNRs (Figure 4b) and to indicate where the information on valence change and structural deformation induced by strain is contained (Figure 4c): fine structures on the Ti L_{23} edge and on the Mn L_{23} edge (in this latter case, the intensity ratio L_3/L_2 is a good indicator of any valence change).

In a very recent study, Garcia et al.[17] have demonstrated that a non-volatile control of spin polarization in an MTJ can be achieved by replacing the insulator in the barrier with a ferroelectric and taking advantage of its hysteretic polarization under the control of an electric field. Practically, the magnetoelectric coupling is realized between the ferromagnetic electrodes (LSMO and Fe) through a ferroelectric thin barrier of barium titanate (BTO for $BaTiO_3$). Mechanisms at the origin of this modulation were theoretically predicted based on interfacial effects, so that refined electron microscopy and spectroscopy investigations with atomic resolution, were required at the relevant interfaces.

For this purpose, an LSMO/BTO /Fe sandwich was grown, so that the interface properties could be investigated in detail. While the BTO film is epitaxially grown on top of LSMO (see its orientation in Figure 5), the Fe layer consists of textured nanocrystallites. The interplanar distance, for selected crystallites in the Fe layer, i.e. ~2.03 Å, is consistent with the {011} planes of b.c.c. Fe. Both bright field (BF) and HAADF images confirm, with atomic spatial resolution, the perfect structure of the BTO layer, free of interface defects. The interpretation of the HAADF is much more straightforward and does not require intensive image simulations when atoms in the crystal structure have very dissimilar atomic numbers. The perovskite A-type atomic columns (Ba atoms) are clearly visible as whiter spots and their presence can unambiguously be detected up to the last plane before the interface.

As subtle structural, chemical, and /or electronic modifications may be expected to occur at the interface, it is interesting to illustrate how these effects are explored using a combination of simultaneously acquired structural and elemental maps, with the support of theoretical simulations. In Figure 6, one can see: (a) one of the possible models for a perfect interface between BTO and Fe, in which Fe atoms may substitute for Ba atoms at the interface layer, (b) the theoretical image simulations, and (c and d) experimental HAADF images (seen as a three-dimensional intensity view or its two-dimensional black and white projection, respectively). These structural images just reveal the position of the Ti columns, as features of very weak intensity between the Ba atomic columns along the [001] direction, and a small elongation of the ultimate Ba interlayer separation with respect to the bulk inter-reticular distance. In Figure 6e, elemental profiles deduced from an EELS spectrum-image after background subtraction and summation over the vertical pixel lines, are superposed on the similarly acquired and processed HAADF profile. In this chemical analysis, the Ti columns now appear clearly between the Ba columns, there is a hint of superposition between Ba and Fe signals at the apex of the interface plane. In the previous paper,[17] it was stated that according to the XAS, HRTEM, and STEM analysis, the Fe

/BTO interface is smooth with no detectable oxidation of the Fe layer within a limit of less than one nanometer. In our most recent analysis, the variation in O-K signal and the apparent changes in Fe white line fine structures suggest the presence of oxygen-iron bonding in this area, which can be naturally explained by the occurrence of a non-negligible number of O-Fe bonds, as visible in Figure 6a. A more comprehensive study involving a comparison with different structural models resulting from ab initio calculations is in preparation.[18]

CONCLUSION

This short review is intended to carry two messages. The first one is that most recent advances in electron microscopy instrumentation and methods have opened a wide field of refined investigation, as demonstrated with a couple of situations involving interfaces in functional hetero-structures. The fine probe of electrons can explore the neighborhood of a solid interface oriented parallel to the beam direction, atomic column by atomic column. The various signals available allow one to analyze unambiguously, at the same level of spatial resolution, the chemical nature of the atoms present and furthermore, their local crystallographic and electronic environment.

The second message is that these developments require in parallel equivalent progress in numerical tools for ab initio modeling of the structures and for processing the vast amount of recorded data.

The successful growth of quasi-perfect interfaces in oxide hetero-structures has opened the gateway to a very exciting class of new compounds with remarkable properties. There is therefore plenty of room for future studies in interface characterization with the highest resolution and sensitivity.

ACKNOWLEDGEMENTS

Thanks are due to all our colleagues in the Orsay STEM group for permanent assistance and stimulating discussions. The present work has used the Nion UltraSTEM microscope acquired with the financial support of CNRS and Essonne region. Finally, the authors acknowledge the European Union under the Framework 6 program for a contract as an Integrated Infrastructure Initiative Reference 026019 ESTEEM.

References

1. F. Pailloux, D. Imhoff, T. Sikora, A. Barthélémy, J.-L. Maurice, J.-P. Contour, C. Colliex, and A. Fert, *Phys. Rev. B,* 66 (2002), 014417.
2. M. Bowen, J.-L. Maurice, A. Barthélémy, M. Bibes, D. Imhoff, V. Bellini, R. Bertacco, D. Wortmann, P. Seneor, E. Jacquet, A. Vaurès, J. Humbert, J.-P. Contour, C. Colliex, S. Blügel, and P.H. Dederichs, *J. Phys.: Condens. Matter,* 19 (2007), 315208.
3. O.L. Krivanek, G.J. Corbin, N. Dellby, B.F. Elston, R.J. Keyse, M.F. Murfitt, C.S. Own, Z.S. Szilagyi, and J.W. Woodruff, *Ultramicroscopy,* 108 (2008), pp. 179–195.
4. O.L. Krivanek, M.F. Chisholm, V. Nicolosi, T.J. Pennycook, G.J. Corbin, N. Dellby, M.F. Murfitt, C.S. Own, Z.S. Szilagyi, M.P. Oxley, S.T. Pantelides, and S. J. Pennycook, *Nature,* 464 (2010), p. 571.
5. C. Jeanguillaume and C. Colliex, *Ultramicroscopy,* 28 (1989), p. 252.
6. C. Colliex, N. Brun, A. Gloter, D. Imhoff, K. March, C. Mory, O. Stéphan, M. Tencé, and M. Walls, *Phil. Trans. Royal Society A,* 367 (2009), p. 3845.
7. R. Arenal, F. de la Peña, O. Stéphan, M. Walls, M. Tencé, A. Loiseau, and C. Colliex, *Ultramicroscopy,* 109 (2008), p. 32.
8. N. Bonnet, N. Brun, and C. Colliex, *Ultramicroscopy*, 77 (1999), p. 97.
9. F de la Peña, M.-H. Berger, J.-F. Hochepied, F. Dynys, O. Stephan, and M. Walls, *Ultramicroscopy* (in press).
10. A. Gloter, A. Douiri, M. Tencé, and C. Colliex, *Ultramicroscopy,* 96 (2003), p. 385.
11. K. Kimoto, T Asaka, T. Nagai, M. Saito, Y. Matsui, and K. Ishizuka, *Nature,* 450 (2007), p. 702.
12. M. Bosman, V. Keast, J.L. Garcia-Munoz, A.J. D'Alfonso, S.D. Findlay, and L.J. Allen, *Phys. Rev. Lett.,* 99 (2007), 086102.
13. D.A. Muller, L. Fitting Kourkoutis, M. Murfitt, J.H. Song, H.Y. Hwang, J. Silcox, N. Dellby, and O.L. Krivanek, *Science,* 319 (2008), p. 1073.
14. J.-L. Maurice, D. Imhoff, J.-P. Contour, and C. Colliex, *Phil. Mag.*, 86 (2006), p. 2127.
15. S. Estradé, J. Arbiol, F. Peiro, I.C. Infante, F. Sanchez, J. Fontcuberta, F. De la Peña, M. Walls, and C. Colliex, *Appl. Phys. Lett.,* 93 (2008), 112505.
16. S. Estradé, J.M. Rebled, M.G. Walls, F. de la Peña, C. Colliex, R. Cordoba, I.C. Infante, G. Herranz, F. Sanchez, J. Fontcuberta, and F. Peiro, "Electron Stability of Burried (001) and (110) $SrTiO_3$ / $La_{2/3}Ca_{1/3}MnO_3$ Interfaces," submitted to *Advanced Materials* (2010).
17. V. Garcia, M. Bibes, L. Bocher, S. Valencia, F. Kronast, A. Crassous, X. Moya, S. Enouz-Vedrenne, A. Gloter, D. Imhoff, C. Deranlot, N. D. Mathur, S. Fusil, K. Bouzehouane, and A. Barthélémy, *Science,* 327 (2010), p. 1106.
18. L. Bocher et al., "Atomic and Electronic Interface Structure of Multiferroic Tunnel Junctions," in preparation (2010).

Christian Colliex, Laura Bocher, Francisco de la Peña, Alexandre Gloter, Katia March, and Michael Walls are with Laboratoire de Physique des Solides (UMR CNRS 8502), Bâtiment 510, Université Paris Sud XI, 91405 Orsay, France. Dr. Colliex can be reached at colliex@lps.u-psud.fr.